Journal of Crystal Growth 311 (2009) 2116–2119

Contents lists available at ScienceDirect

Journal of Crystal Growth

journal homepage: www.elsevier.com/locate/jcrysgro

MBE growth of II–VI materials on GaSb substrates for photovoltaic applications

S. Wang [a], D. Ding [a], X. Liu [b], X.-B. Zhang [c], D.J. Smith [d], J.K. Furdyna [b], Y.-H. Zhang [a,*]

[a] Center for Nanophotonics and Department of Electrical Engineering, Arizona State University, Tempe, AZ 85287, USA
[b] Department of Physics, University of Notre Dame, Notre Dame, IN 46556, USA
[c] School of Materials, Arizona State University, Tempe, AZ 85287, USA
[d] Department of Physics, Arizona State University, Tempe, AZ 85287, USA

ARTICLE INFO

Available online 11 October 2008

PACS:
61.05.cp
78.55.Et
68.37.Og
81.15.Hi

Keywords:
A1. X-ray diffraction
A3. Molecular beam epitaxy
B2. Semiconducting II–VI materials
B3. Solar cells

ABSTRACT

The II–VI materials lattice matched to GaSb substrates are desirable for ultrahigh-efficiency multijunction solar cells. This paper reports the growth of ZnTe and ZnCdTe/ZnTe quantum wells on undoped GaSb (1 0 0) substrates using molecular beam epitaxy. During growth, *in situ* reflection high-energy electron diffraction shows fast and smooth transition from GaSb surface to ZnTe surface. Post-growth structural characterization using X-ray diffraction and high-resolution transmission electron microscopy reveals very low-defect density, i.e. high crystalline quality. Visible photoluminescence is observed from 10 to 300 K.

1. Introduction

The II–VI (MgZnCd)(SeTe) materials have direct bandgaps and can be grown lattice matched on 6.1 Å III–V substrates such as GaSb and InAs. It was proposed recently that their integration with (AlGaIn)(AsSb) materials offers an ideal material system for photovoltaic applications because this would cover the entire solar spectrum from 3.0 down to 0.4 eV [1]. Since some II–VI materials are nearly lattice matched to the 6.1 Å III–V substrates, epitaxial layers grown on those substrates are expected to generate very low-density misfit dislocations. This innovative approach would enable multijunction solar cells made of this hetero-valent material system to have a large number of junctions with minimum defect densities, which would significantly improve the overall energy conversion efficiency. It is also known that some of the lattice-matched II–VI and III–V interfaces, for example, CdSe/ZnTe and InAs/GaSb, have type-II band-edge alignment, which is desirable for the tunnel junctions between each individual subcell for tandem structures.

A practical design of a high-efficiency 4-junction solar cell consisting of two III–V subcells (GaSb and AlGaAsSb) and two II–VI subcells (CdSeTe and ZnTe) has been recently proposed, with bandgap energies almost evenly distributed from 0.73 to 2.27 eV [1,2]. The bandgap energy of ZnTe (2.27 eV at room temperature) covers the short-wavelength range of the solar spectrum, which contributes substantially (over 25% at AM1.5 G) to the entire solar radiation energy. There is only 0.12% lattice mismatch between ZnTe and GaSb. Moreover, the thermal expansion coefficient of ZnTe ($8.33\times10^{-6}\,K^{-1}$ at 300 K) is very close to that of GaSb ($6.35\times10^{-6}\,K^{-1}$ at 300 K) so that the two materials are also thermally matched [3]. Thus ZnTe is an essential constituent material in the proposed novel multijunction solar cell structures. This paper focuses on growth and characterization of ZnTe and ZnCdTe/ZnTe quantum well structures grown on GaSb.

The growth of ZnTe/GaSb heterostructures has been studied for several decades [4]. Different techniques including RF sputtering [5], metalorganic chemical vapor deposition (MOCVD) [6], and metalorganic vapor phase epitaxy (MOVPE) [7] have been employed to grow ZnTe on GaSb. Molecular beam epitaxy (MBE) has also been used to grow these material systems, such as ZnTe grown with GaSb buffers on GaAs or GaSb substrates [8,9], and ZnTe with AlSb buffer on GaSb substrates [10]. However, it is still very challenging to obtain high-quality materials for device applications such as solar cells. This paper describes the growth of ZnTe layers and ZnCdTe/ZnTe quantum wells on GaSb substrates using MBE, and the study of their structural and optical properties using high-resolution X-ray diffraction (XRD), high-resolution transmission electron microscopy (TEM), and temperature-dependent photoluminescence (PL).

*Corresponding author.
E-mail address: yhzhang@asu.edu (Y.-H. Zhang).

0022-0248/$ - see front matter © 2008 Elsevier B.V. All rights reserved.
doi:10.1016/j.jcrysgro.2008.09.189

2. Experiments

The epitaxial growth is carried out using an MBE system consisting of III–V and II–VI chamber, which are connected with a UHV transfer module. Two sets of samples are grown. The first set consists of thin ZnTe layers grown on GaSb substrates to study the growth conditions and structural properties. The second set is ZnCdTe/ZnTe quantum well structures to study their optical properties using PL. In the quantum well structures, the ZnTe layers provide confinement to the photogenerated carriers to prevent them from recombining non-radiatively at the surface and interfaces. For the growth of ZnTe, undoped GaSb (1 0 0) substrates are first deoxidized in the III–V chamber at 500 °C under an antimony flux with beam equivalent pressure (BEP) around 1.6×10^{-6} Torr, followed by the growth of a GaSb buffer layer (~20 nm) at 480 °C. The substrate temperatures are measured by a thermocouple on the back of substrate holder which is calibrated by a pyrometer facing the holder surface. The samples are cooled down to room temperature and then transferred to the II–VI chamber, where ZnTe layers are grown on the GaSb buffer layers. The growth of ZnTe is initialized under a Zn flux for several seconds prior to opening the Te shutter, to minimize the formation of Ga_2Te_3 phase [11,12]. The substrate temperatures are varied between 300 and 350 °C and the BEP ratios of Zn to Te (around 1:1, depending on the surface reconstruction monitored by RHEED) are adjusted to optimize the growth conditions. For the growth of the ZnCdTe/ZnTe quantum well layer, a thin (5–10 nm) ZnCdTe layer is grown on a thick ZnTe layer (~400 nm) deposited on a GaSb buffer layer. The BEP ratio of Cd to Zn is about 12% during the growth of the ZnCdTe layer. The ZnCdTe layer is capped by a thin ZnTe layer as another confinement layer to form the quantum well structure.

Cross-sectional TEM samples are prepared by mechanical polishing and ion-beam thinning. To minimize thermal damage to the II–VI materials, liquid-nitrogen cooling and low-energy (3 keV) ion beams are used. At the end of the ion-beam thinning, a lower energy (2 keV) ion beam is used to clean the surface. The samples are imaged using a JEOL JEM 4000EX transmission electron microscope with point-to-point resolution of 1.7 Å. The HRTEM images are taken at Scherzer defocus condition. The high-resolution XRD rocking curve characterization is performed using a PANalytical X'Pert PRO MRD X-ray diffractometer with multi-crystal monochromator. The Kα1 emission line of copper (1.54 Å) is used as the incident beam. The X'Pert Epitaxy software is used for simulating the $\omega-2\theta$ data. For characterization of optical properties, temperature-dependent PL measurements are carried out using the 363 or 488 nm lines of an Argon ion laser for excitation and a photomultiplier tube as the detector.

3. Results and discussion

During the growth of ZnTe on GaSb, the evolution of surface reconstruction is monitored *in situ* by RHEED. As shown in Fig. 1, RHEED shows a typical (1×3) reconstruction pattern of the GaSb surface before growth of ZnTe layer. At the beginning of the ZnTe growth, RHEED shows spotty and weakly defined patterns, indicating a transition from (1×3) surface to (1×2) surface. The transition takes as short as 10 s and is caused by the formation of a thin interfacial layer between GaSb and ZnTe. The interfacial layer may consist of various III–VI or II–V compounds such as Ga_2Te_3 and Zn_3Sb_2, as well as GaSb and ZnTe [11]. After the growth of this transition layer, the typical (1×2) ZnTe surface reconstruction RHEED pattern starts to appear. A bright and streaky RHEED pattern with clear (1×2) surface reconstruction remains throughout the rest of the ZnTe growth.

After growth, high-resolution XRD measurements are performed in the vicinity of the (0 0 4) GaSb diffraction peak. The XRD $\omega-2\theta$ results from a single ZnTe layer with nominal thickness of 110 nm determined by the MBE growth rate, reveal distinct peaks for the GaSb substrate and the ZnTe layer (Fig. 2a). Pendellösung fringes are clearly observed, indicating a high-quality single-crystal epitaxial

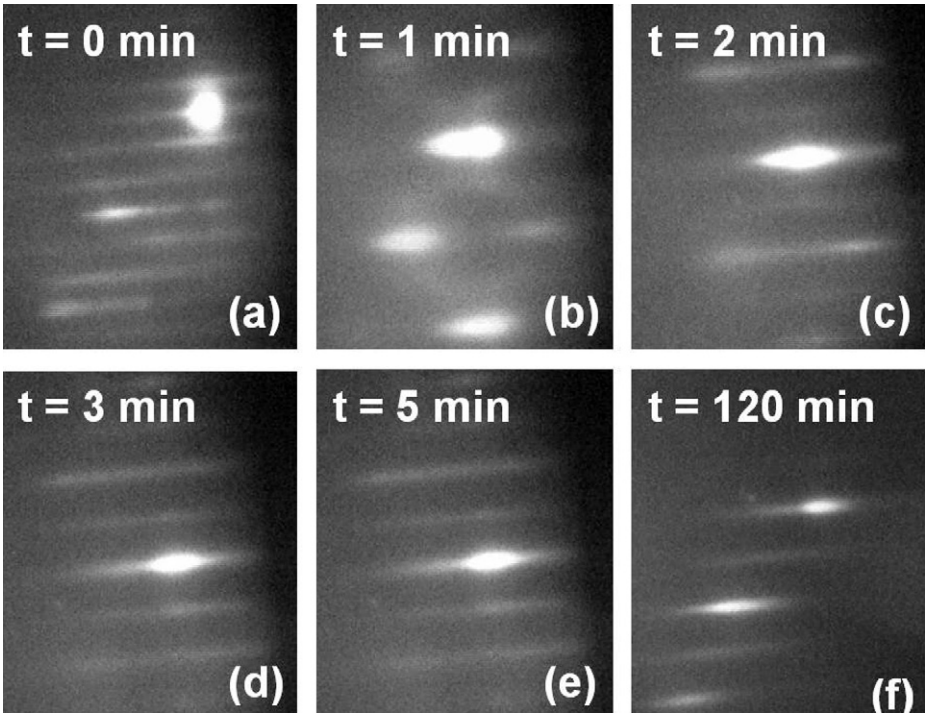

Fig. 1. (a) GaSb (1×3) reconstruction before the growth of ZnTe. (b) Spotty RHEED pattern within the first minute of ZnTe growth on GaSb. (c)–(f) ZnTe (1×2) reconstruction after 1 min growth and longer.

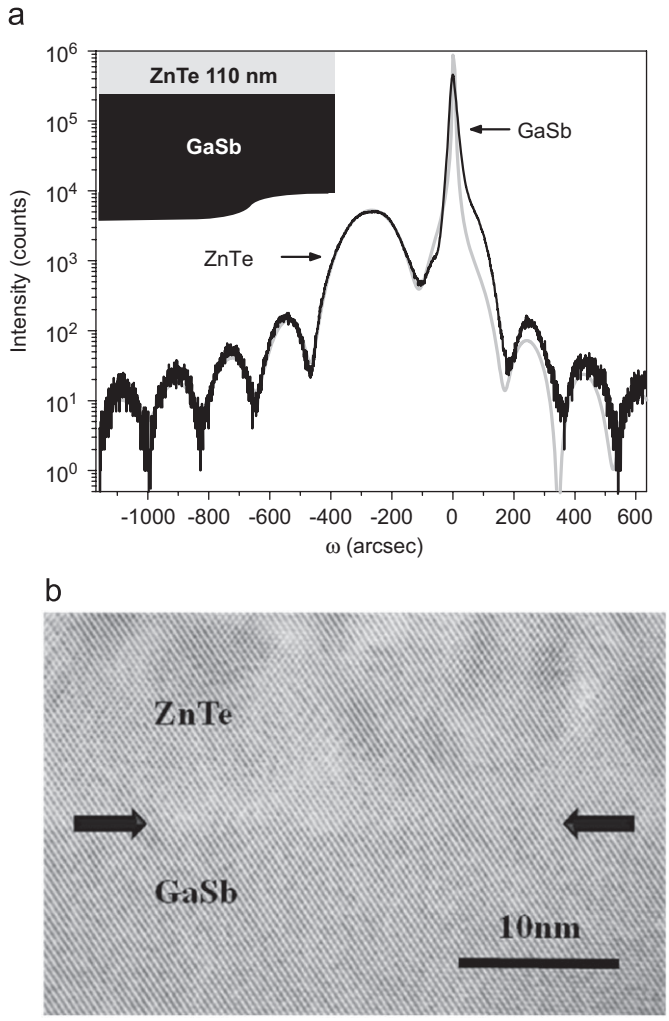

Fig. 2. (a) XRD $\omega-2\theta$ measurements of a single ZnTe layer grown on GaSb substrate, with ω-axis normalized to the (0 0 4) GaSb diffraction peak. Measured data are shown in black and simulation results are shown in gray. The schematic diagram of the sample structure is shown in the inset and (b) TEM image of the same thin ZnTe layer sample, with the arrows pointing to the interface between ZnTe and GaSb.

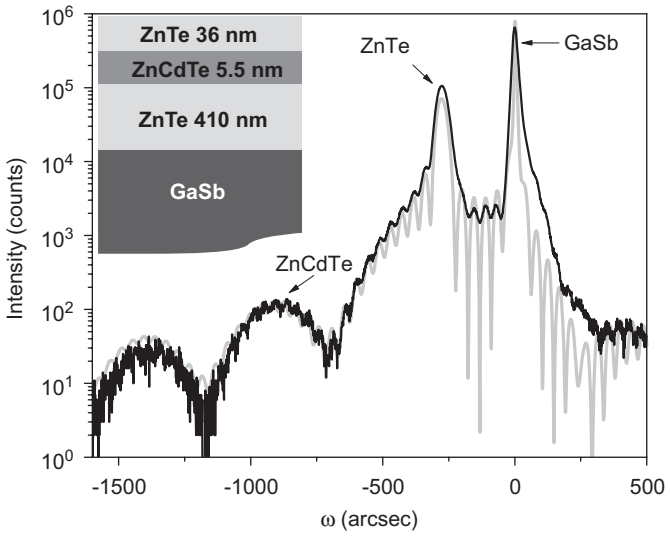

Fig. 3. XRD $\omega-2\theta$ measurements of a $Zn_{0.91}Cd_{0.09}Te$/ZnTe quantum well, with ω-axis normalized to the GaSb [0 0 4] diffraction angle. The schematic diagram of the sample structure is shown in the inset. Measured data are shown in black and simulation results are shown in gray.

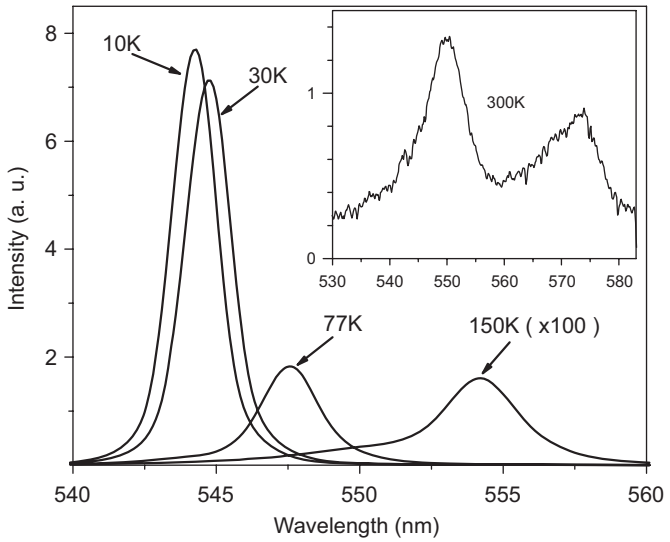

Fig. 4. PL from a ZnCdTe/ZnTe quantum well at different temperatures, with 300 K data shown in inset.

layer with smooth interfaces, uniform thickness, and low-defect density. The layer thickness is determined to be 105 nm from the period of the fringes. For comparison, the simulated $\omega-2\theta$ data are also plotted in Fig. 2a, which gives the ZnTe layer thickness of 105 nm and a strain relaxation of 30%.

The TEM image shown in Fig. 2b of the same single ZnTe layer also indicates excellent crystallinity properties and smooth interfacial configuration between ZnTe and GaSb. This observation reveals that exposure of GaSb to the Zn flux prior to the growth of ZnTe significantly suppresses the formation of any Ga_2Te_3 phase at the interface, which sometimes can be visible in TEM images [13]. Moreover, no misfit dislocations and stacking faults are observed at the ZnTe/GaSb interface in the TEM images. These findings indicate that it is possible to obtain a nearly defect-free interface between ZnTe and GaSb because they have a very small lattice mismatch of 0.12%. In contrast, ZnTe layers grown on GaAs possess high density of 90° and 60° dislocations [14]. The present results also demonstrate significant improvement of the crystalline and interfacial quality of the materials, compared to previous results for ZnTe/GaSb [9].

For the ZnCdTe/ZnTe quantum well sample, the XRD $\omega-2\theta$ results show three main peaks in Fig. 3: the GaSb substrate peak, the ZnTe peak, and the ZnCdTe peak. The positions of the main peaks are used to estimate the lattice constant of ZnTe (6.10371 Å) and ZnCdTe (6.13544 Å), from which the Cd composition is determined to be 9.2%. Pendellösung fringes are also clearly observed, indicating excellent crystalline quality, uniform composition, and smooth interfaces. The simulation is also shown in Fig. 3, which gives a thickness of 410 nm for the ZnTe buffer layer, 5.5 nm for the ZnCdTe quantum well layer, and 36 nm for the ZnTe cap layer.

The PL measurements are carried out on the above ZnCdTe/ZnTe quantum well sample, and the spectra are shown in Fig. 4. PL peaks from the ZnCdTe quantum well are observed from 10 to 150 K, while the 300 K data (the inset of Fig. 4) show both peaks from the ZnCdTe quantum well (λ=570 nm) and the ZnTe barrier layer (λ=550 nm). At low temperatures there is an emission from the ZnTe barrier layer as well, but it is less visible compared to the emission from the well that is much stronger in intensity and decreases rapidly with increasing temperature. The red shift of the PL peaks can be explained by the temperature dependence of the

bandgap energies. The measured ZnCdTe bandgap energy of 2.18 eV at 300 K indicates a 9.1% Cd mole fraction, which is in good agreement with that (9.2%) obtained by the XRD measurements.

In summary, we have demonstrated successful MBE growth of nearly lattice-matched ZnTe and ZnCdTe/ZnTe quantum well structures on GaSb substrates with excellent structural and optical properties. High-resolution XRD results show clear Pendellösung fringes and the simulation fits the experimental data very well. No dislocations or stacking faults are observed at the ZnTe/GaSb interface from high-resolution TEM images. Visible PL is observed from 10 to 300 K. It is therefore reasonable to conclude that these materials grown on GaSb substrates should be suitable for photovoltaic and other optoelectronic device applications.

Acknowledgements

The authors gratefully acknowledge the use of facilities in the John M. Cowley Center for High-Resolution Electron Microscopy, the Center for Solid State Electronics Research, and the LeRoy Eyring Center for Solid State Science at Arizona State University. This work is supported by the Science Foundation Arizona with Contract no. SRG 0190-07.

References

[1] Y.-H. Zhang, S.-Q. Yu, S.R. Johnson, D. Ding, S.-N. Wu, in: Proceedings of the 33rd IEEE Photovoltaic, Energy Specialist Conference, 2008, in press.
[2] S.-N. Wu, D. Ding, S. R. Johnson, S.-Q. Yu, Y.-H. Zhang, unpublished.
[3] S. Adachi, Properties of Group-IV III–V and II–VI Semiconductors, Wiley, West Sussex, England, 2005.
[4] S. Kamuro, C. Hamaguchi, M. Fukushima, J. Nakai, Solid State Electron. 14 (1971) 1183.
[5] Y. Tokumitsu, A. Kawabuchi, H. Kitayama, T. Imura, Y. Osaka, F. Nishiyama, J. Appl. Phys. 66 (1989) 896.
[6] H. Dumont, J.-E. Bourée, A. Marbeuf, O. Gorochov, J. Crystal Growth 130 (1993) 600.
[7] H. Leiderer, G. Jahn, M. Silberbauer, W. Kuhn, H.P. Wagner, W. Limmer, W. Gebhardt, J. Appl. Phys. 70 (1991) 398.
[8] Y. Rajakarunanayake, B.H. Cole, J.O. McCaldin, D.H. Chow, J.R. Söderström, T.C. McGill, C.M. Jones, Appl. Phys. Lett. 55 (1989) 1217.
[9] C.T. Chou, J.L. Hutchison, D. Cherns, M.-J. Casanove, J.W. Steeds, R. Vincent, B. Lunn, D.A. Ashenford, J. Appl. Phys. 74 (1993) 6566.
[10] D.L. Mathine, S.M. Durbin, R.L. Gunshor, M. Kobayashi, D.R. Menke, Z. Pei, J. Gonsalves, N. Otsuka, Q. Fu, M. Hagerott, A.V. Nurmikko, Appl. Phys. Lett. 55 (1989) 268.
[11] C.R. Li, B.K. Tanner, D.E. Ashenford, J.H.C. Hogg, B. Lunn, J. Appl. Phys. 82 (1997) 2281.
[12] M.P. Halsall, D. Wolverson, J.J. Davies, B. Lunn, D.E. Ashenford, Appl. Phys. Lett. 60 (1992) 2129.
[13] R.J. Miles, J.F. Swenberg, M.W. Wang, M.C. Phillips, T.C. McGill, J. Crystal Growth 138 (1994) 523.
[14] T.W. Kim, D.U. Lee, H.S. Lee, J.Y. Lee, H.L. Park, Appl. Phys. Lett. 78 (2000) 1409.